First order phase transition in deuterated triglycine selenate under an electric field: experimental study and analysis in the frame of Landau theory

2009 J. Phys.: Condens. Matter 21 155902

(http://iopscience.iop.org/0953-8984/21/15/155902)

J. Phys.: Condens. Matter **21** (2009) 155902 (7pp) doi:10.1088/0953-8984/21/15/155902

First order phase transition in deuterated triglycine selenate under an electric field: experimental study and analysis in the frame of Landau theory

F J Romero, M C Gallardo and J del Cerro

Departamento de Física de la Materia Condensada, Instituto Mixto de Ciencia de Materiales
CSIC-Universidad de Sevilla, Apartado 1065, 41080 Sevilla, Spain

E-mail: fjromero@us.es

Received 9 September 2008, in final form 19 February 2009
Published 20 March 2009
Online at stacks.iop.org/JPhysCM/21/155902

Abstract
The influence of electric fields lower than the critical field in the ferroelectric phase transition in deuterated triglycine selenate has been studied by means of thermal and dielectric properties. The latent heat, specific heat and dielectric constant have been measured and compared to the theoretical expectations from the Landau theory under an electric field. A full agreement has been found on cooling experiments.

1. Introduction

First order ferroelectric phase transitions are characterized by discontinuities in the polarization P, the enthalpy (exhibiting latent heat L), the specific heat c and the dielectric susceptibility χ at the transition temperature. They may also show stable and metastable regions and thermal hysteresis as a consequence. The discontinuities are influenced by the electric field E, since it is the conjugated field of the order parameter. For electric fields higher than a critical value E_{cr} the discontinuities would disappear.

Landau's theory has been extensively used to describe phase transitions in ferroelectric materials at zero electric field. The influence of the electric field is accounted for by adding $-EP$ in the free energy series expansion. On the other hand, the study of thermal properties, such as specific heat and latent heat, under an electric field and its comparison to theoretical models is unusual, unlike dielectric properties. As an example, studies of the second order phase transition in triglycine sulfate (TGS) [1, 2], the tricritical phase transition in triglycine selenate (TGSe) [3, 4] and the first order phase transition in KDP [5–7] should be mentioned.

Theoretical analysis of the phase diagram under an electric field, including the width of the stable and metastable limits, has been outlined [8–10] in the case of first order phase transitions below the critical field. Yet no detailed comparison of these predictions to experimental data of specific heat and latent heat can be found in the literature for any material.

The absence of these kinds of studies is probably related to the fact that high precision calorimetry is necessary for a comprehensive study of the influence of the electric field on specific heat and latent heat in a first order phase transition below the critical field. The key point here is that the electric field must not distort the measuring process. On the other hand, the calorimeter technique should provide sufficiently accurate data to ascertain the influence of the applied electric field.

The determination of low latent heats is one of the most significant tasks at this point. Well known methods such as differential scanning calorimetry (DSC) or differential thermal analysis (DTA) actually measure change of enthalpy. This change of enthalpy has two contributions: one due to the specific heat variation with the temperature and another due to the latent heat. The experimental method must discriminate both contributions, if a precise latent heat measurement is required.

An original technique, based on conduction calorimetry, was developed by our group [11]. The technique is able to measure absolute values of specific heat and accurate latent heat. It is powerful when the latent heat contribution is comparatively small while the specific heat is showing a divergence, as in the case of a phase transition close to a tricritical point. Furthermore, electric field or uniaxial stress can be applied during the measuring process. The

technique was successfully used for the study of ferroelectric and ferroelastic materials under electric field and uniaxial stress, respectively [6, 12].

The absence of these kinds of studies could be also related to the lack of appropriate materials. Deuterated triglycine selenate, $TGSe_{1-x}DTGSe_x$, provides a very interesting material for performing the previously outlined analysis.

The ferroelectric phase transition in the non-deuterated material, TGSe, is one of the best examples of a system following a classical tricritical Landau behaviour, and the coefficients of the corresponding 2-6 potential have been determined [13]. The tricritical behaviour makes significant the influence of different parameters, such as electric field, uniaxial stress or deuteration on the nature of the phase transition.

The transition was found to become discontinuous after sample deuteration [14–16]. In a previous work [17], the phase transition in an almost fully deuterated (90%) sample of TGSe at zero electric field was characterized by measuring specific heat, latent heat and dielectric susceptibility. The whole set of experimental data was successfully described by a 2-4-6 Landau potential for the free energy whose coefficients were also determined. It would be very interesting to perform these measurements under electric fields below and above the critical field. However, the critical field is estimated to be 5500 V cm^{-1}, which is much higher than the available values for our device.

In this work we study the influence of electric fields lower than the critical field on the phase transition in a 90% deuterated TGSe sample by precise specific heat, latent heat and dielectric susceptibility measurements. Experimental data under an electric field will be discussed in the framework of the Landau theory.

2. Experimental details

A single crystal of deuterated TGSe was prepared at the Institute of Physics, Adam Mickiewicz University, Poznan, Poland and it is the same used in the analysis of the zero-field behaviour [17]. The degree of deuteration was estimated to be 90% from the relation given by Gesi [14]. The sample was 2.55 mm thick and had a mass of 0.35 g. Its main faces, with a pseudo-hexagonal cross-section equal to 71 mm^2, were prepared perpendicular to the *b*-axis with gold electrodes evaporated on them.

The calorimetric measurements were carried out in a high-resolution conduction calorimeter previously described in detail [18], which allows an electric field to be applied on the sample. The maximum voltage across the electrodes is 200 V due to the low electrical insulation in the wires, which, on the other hand, provides a high thermal anchorage with the calorimetric block. The corresponding maximum electric field is 800 V cm^{-1} considering the sample geometry.

The absolute value of the specific heat is obtained by integrating the electromotive force given by two heat fluxmeters when the temperature of the sample changes as a consequence of the superposition of a long-periodic serial of square thermal pulses to a heating or cooling ramp [19].

In a second experiment, the equipment worked as a high sensitivity DTA device. The large number of thermocouples in each fluxmeter and the high thermal stability allow a temperature variation rate similar to that used in heat capacity measurements while keeping a low noise signal. Latent heat is evaluated by the comparison of DTA trace with specific heat data following the method described previously [20].

The dielectric constant was measured using a ESI-SP 5400 capacitance bridge at a frequency of 1 kHz in a cell different to that used to get the data on thermal properties.

3. Experimental results

3.1. Specific heat

The specific heat was measured on cooling and heating runs for $E = 400$ and 800 V cm^{-1} at a scanning temperature rate of 0.03 K h^{-1}. A point was obtained each 0.01 K, providing a great number of data close to the transition point. The relevant magnitude to make a comparison with a theoretical model for a phase transition is the specific heat excess Δc, obtained from subtraction of an appropriate baseline. The baseline determined for data at $E = 0$, which is a linear extrapolation of the specific heat of the paraelectric phase [17], was used for this purpose.

Figure 1 shows Δc versus temperature on cooling and heating runs for $E = 0$, 400 and 800 V cm^{-1} in a temperature interval of 5 K around the transition temperature. For $E = 0$ the transition was found to take place in two stages divided by a phase coexistence interval, when both phases coexist without transformation due to the presence of an internal break across the sample [17]. For the sake of clarity, only monophase states (either ferroelectric or paraelectric) are shown in figure 1.

For $E = 0$, the specific heat on heating runs behaves as data in a cooling experiment, although the transition takes place at a higher temperature showing thermal hysteresis, in agreement with the first order nature of the phase transition.

On the contrary, data for heating runs under an electric field do not follow the behaviour observed for data on cooling runs and a systematic deviation is found close to the transition temperature. It is noteworthy that a similar behaviour was observed in the tricritical phase transition of non-deuterated TGSe [13] where data on heating and cooling runs were found to match to each other for a zero-field experiment. On the other hand, they differ within a narrow temperature interval of 0.2 K around the transition temperature for applied electric fields lower than 175 V cm^{-1} [21]. A similar behaviour was also observed after a uniaxial pressure was applied along the ferroelectric axis in TGSe [13].

The temperature at the maximum of the specific heat anomaly is shown in figure 2. It increases as electric field increases on cooling and heating runs. For each electric field, the sample undergoes ferroelectric to paraelectric phase transition at a higher temperature than the corresponding value for the paraelectric to ferroelectric phase transition, in agreement with a first order phase transition.

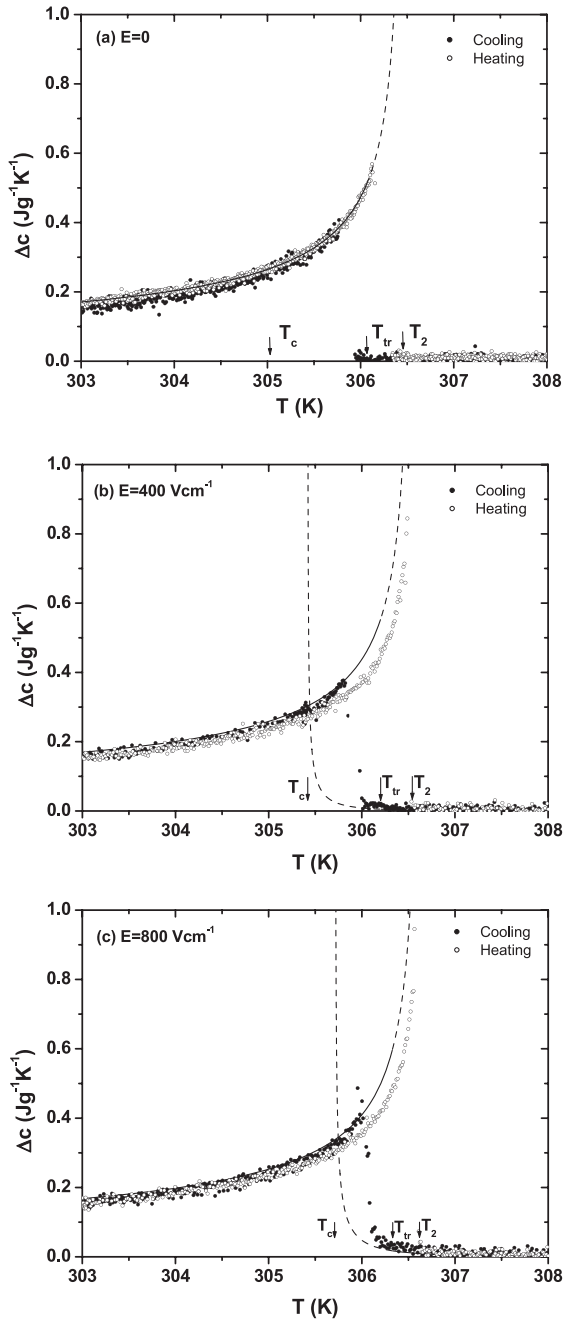

Figure 1. Specific heat excess versus temperature for (a) $E = 0$, (b) $E = 400$ V cm^{-1} and (c) $E = 800$ V cm^{-1}, on cooling runs (solid circles) and heating runs (open circles). The predictions computed from the Landau theory are also shown: solid lines for stable values and dashed lines for metastable values. Calculated characteristic temperatures are shown by arrows.

3.2. Latent heat

The enthalpy discontinuity at the transition was obtained by integrating the DTA trace after subtracting a baseline determined from the specific heat data following a procedure developed by our group [20] and previously applied for zero-field measurements in this sample [22]. For each of the electric fields, two values for the latent heat—heating run L_h and cooling run L_c—were obtained. Data are summarized in table 1.

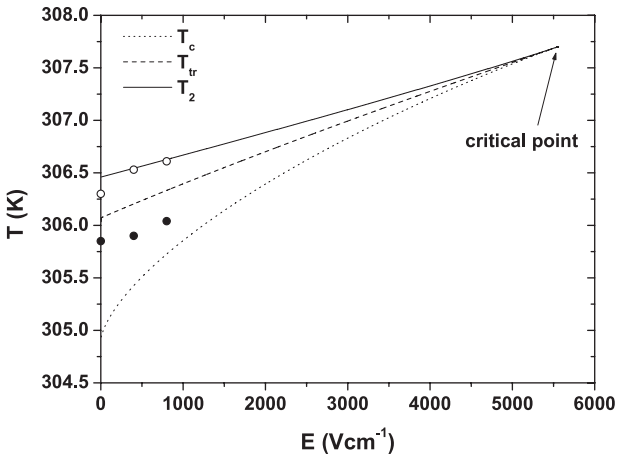

Figure 2. Temperature of the maximum of the specific heat T_m versus applied electric field on cooling runs (solid circles) and heating runs (open circles). ET phase diagram computed from equations (1) and (2), as explained in the text, is also shown. The boundaries of the phase diagram are: T_c, the lowest temperature at which the paraelectric phase may exist, and T_2, the highest temperature at which the ferroelectric phase may exist. The equilibrium phase transition temperature T_{tr} is also shown.

Table 1. Latent heat as a function of the applied electric field on heating runs (L_h) and cooling runs (L_c).

E (V cm^{-1})	L_h (J g^{-1})	L_c (J g^{-1})
0	1.08	1.32
400	0.71	1.28
800	0.68	1.19

Data in table 1 show that the latent heat decreases as the electric field increases. $L_c(E)$ is greater that $L_h(E)$ in any case. On the contrary, the excess specific heat during heating is larger than cooling (see figure 1) and contributes more to the enthalpy. Thus, in order to maintain an enthalpy balance, L must be smaller during heating than during cooling, as observed.

3.3. Dielectric susceptibility

Dielectric susceptibility data for $E = 400$ and 800 V cm^{-1} on cooling and heating runs at a temperature scanning rate of 0.5 K h^{-1} are shown in figure 3. Despite the rate of temperature variation in specific heat measurements being much lower (0.03 K h^{-1}) and the measurements being performed in different devices, the difference between the temperature at the maximum of the dielectric susceptibility anomalies and the temperature at maximum specific heat anomaly was only 0.3 K.

4. Analysis in the framework of the Landau theory under an electric field

4.1. Overview and phase diagram

The phase transition of 90% deuterated TGSe at zero electric field was successfully described [17] in the framework of a

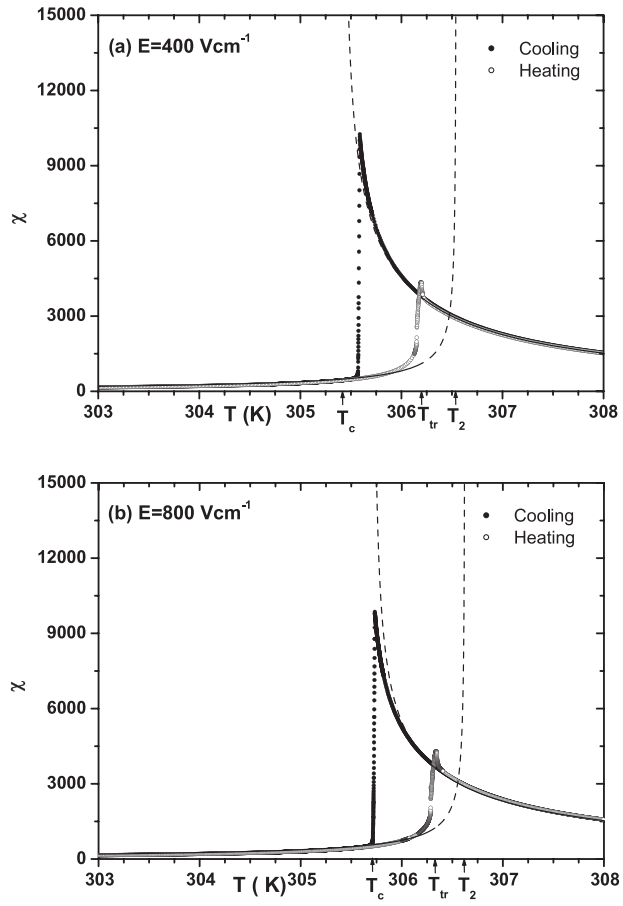

Figure 3. Dielectric susceptibility versus temperature for (a) $E = 400$ V cm^{-1} and (b) $E = 800$ V cm^{-1}, on cooling runs (solid circles) and heating runs (open circles). The predictions from the Landau theory are shown by solid lines for the stable region (note that continuous lines are overlapped by experimental data) and by dashed lines for the metastable region. The characteristic temperatures are shown by arrows.

2-4-6 Landau potential whose thermodynamic potential is

$$\Delta G = \tfrac{1}{2}\alpha(T - T_c^0)P^2 + \tfrac{1}{4}\beta P^4 + \tfrac{1}{6}\gamma P^6 \qquad (1)$$

where the coefficients are $\alpha = 2.40 \times 10^7$ J^{-1} V^2 m K^{-1}, $\beta = -1.8 \times 10^{11}$ J^{-3} V^4 m^5, $\gamma = 2.32 \times 10^{14}$ J^{-5} V^6 m^9 and $T_c^0 = 304.91$ K.

The influence of the electric field is introduced by adding $-EP$ in equation (1). The real solutions of the equation of state,

$$E = \alpha(T - T_c^0)P + \beta P^3 + \gamma P^5, \qquad (2)$$

provide the equilibrium polarization at each temperature under an electric field. A typical temperature dependence of P^2 for $E < E_{cr}$ and the corresponding one for $E = E_{cr}$ are shown in figure 4.

Since this transition is a first order phase transition, hysteresis, related to supercooling and superheating, is expected when analysing the solutions of the equation (2), which may lead either to an absolute minimum (stable state) or to a relative minimum (metastable state) in ΔG. Limits of stability and metastability can be found after analysing these minima.

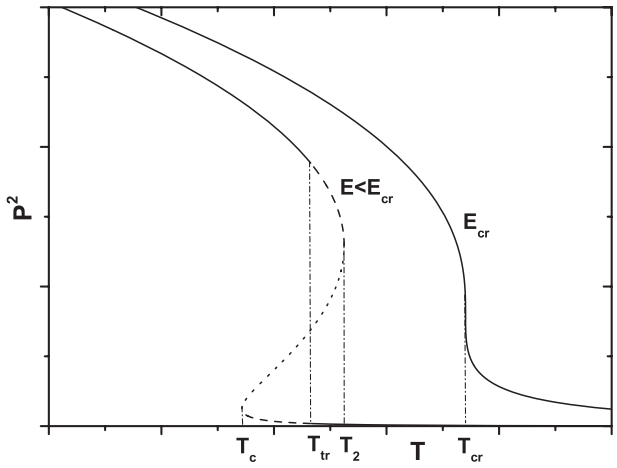

Figure 4. Evolution of squared order parameter versus temperature for $E < E_{cr}$ and $E = E_{cr}$ showing stable states (solid lines), metastable states (dashed lines) and unstable states (dotted lines). The characteristic temperatures for $E < E_{cr}$ and the critical temperature T_{cr} are also shown.

It is convenient to define three characteristic temperatures T_2, T_{tr} and T_c (listed from higher to lower) to delimit the stable and metastable regions for each root. T_2 is the highest temperature at which the low temperature phase could exist. Correspondingly, T_c is the lowest temperature at which the high temperature phase could exist. Finally, T_{tr} is the phase equilibrium temperature, i.e. when $\Delta G_{para} = \Delta G_{ferro}$ and both phases get the same free energy. T_2 and T_c limit theoretically the region where both phases may coexist. The extent of this interval $d = T_2 - T_c$ represents the maximum thermal hysteresis, although the experimental value is generally lower than the theoretical one.

The phase diagram is obtained from the evolution of these temperatures as a function of the electric field. In the limit case for $E = 0$, T_c equals T_c^0 in equation (1) and the values of T_2, T_{tr} and T_c are related by $T_2^0 - T_c^0 = 4(T_2^0 - T_{tr}^0) = \beta^2/(4\alpha\gamma)$, yielding $T_{tr}^0 = 306.07$ and $T_2^0 = 306.46$ K. The superscript stresses the zero-field condition.

For $E \neq 0$, an algorithm similar to that shown by Courtens and Gammon [9] was followed. $P^2(T)$ is computed by introducing the coefficients $\alpha, \beta, \gamma, T_c^0$ (previously computed for $E = 0$) and E in equation (2). The stability limits T_2, and T_c then occurs when the solution of equation (2) is also an inflection point for ΔG, which is mathematically given by solving $dT/dP^2 = 0$. These points are shown in figure 4. T_{tr} is obtained by computing $\Delta G(T, E)$ after introducing the solutions for P^2 from equation (2) and then determined by solving $\Delta G_{ferro}(T_{tr}, E) = \Delta G_{para}(T_{tr}, E)$.

The three characteristic temperatures converge at the critical field, where the line of first order phase transitions is ending. Critical point coordinates are obtained from

$$\frac{d\Delta G}{dP} = \frac{d^2\Delta G}{dP^2} = \frac{d^3\Delta G}{dP^3} = 0 \qquad (3)$$

or

$$\frac{dE}{dP} = \frac{d^2E}{dP^2} = 0 \qquad (4)$$

which yields

$$P_{\rm cr}^2 = -\frac{3\beta}{10\gamma} \tag{5}$$

$$T_{\rm cr} = T_{\rm c}^0 + \frac{9}{20}\frac{\beta^2}{\alpha\gamma} \tag{6}$$

$$E_{\rm cr} = \frac{6\sqrt{3}}{25\sqrt{10}}\frac{(-\beta)^{5/2}}{\gamma^{3/2}}. \tag{7}$$

For 90% deuterated TGSe, the critical point is $P_{\rm cr} = 0.155$ C m^{-2}, $T_{\rm cr} = 307.71$ K and $E_{\rm cr} = 5562$ V cm^{-1}, so that the experiments with $E = 400$ and 800 V cm^{-1} would lie in the first order region.

The comparison of the theoretical model to the experimental data is started by analysing the phase diagram. Following the above described method, the evolution of the characteristic temperatures as a function of the electric field was determined. The corresponding ET phase diagram for this material is shown in figure 2, where a reduction in the coexistence interval as the electric field increases is observed.

It should be pointed out that thermal hysteresis still appears in these experiments despite the low rate of temperature change imposed on them. The transition does not actually take place in phase equilibrium (that is at $T_{\rm tr}$). On cooling, the paraelectric phase is metastable from $T_{\rm tr}$ to $T_{\rm c}$ and the transition occurs at any temperature within this interval. On heating, the ferroelectric phase is metastable from $T_{\rm tr}$ to T_2 and the transformation occurs at any temperature within this interval.

The experimental transition temperature on cooling runs (paraelectric to ferroelectric phase transition) falls within the interval delimited by $T_{\rm tr}$ and $T_{\rm c}$ (see figure 2) in agreement with expectations. Contrastingly, on heating runs, the transition temperature for $E = 0$ reaches an intermediate value from $T_{\rm tr}$ to T_2 but, as the electric field increases, the transition temperature also increases, being shifted toward the boundary T_2. Thus, on heating runs, E makes the ferroelectric phase stable at higher temperatures.

4.2. Specific heat

The specific heat at constant electric field is given by

$$\Delta c = -T\frac{\partial^2 \Delta G}{\partial T^2} = -\alpha T P\frac{\partial P}{\partial T}. \tag{8}$$

By assuming $\partial E/\partial T = 0$ in equation (2):

$$\frac{\partial P}{\partial T} = -\frac{\alpha P}{\alpha(T - T_{\rm c}) + 3\beta P^2 + 5\gamma P^4} \tag{9}$$

and then the specific heat as a function of T and P equals

$$\Delta c(T, P) = \frac{\alpha^2 P^2 T}{\alpha(T - T_{\rm c}) + 3\beta P^2 + 5\gamma P^4}. \tag{10}$$

$\Delta c(T, E)$ cannot be written in the same analytical way. It should be pointed out that it is this $\Delta c(T, E)$ that is significant for discussing the experimental data obtained by varying T under constant E. As an alternative, an approximate numerical computation can be deduced by introducing the real roots of equation (2) into (10). It should be also mentioned that each root gets its own range of stability (and metastability) following the phase diagram shown in figure 2, thus providing stable and metastable values for the specific heat.

The results of this computation for $E = 0$ [17] and for $E = 400$ and $E = 800$ V cm^{-1} are shown in the figure 1. The corresponding characteristic temperatures are also presented in figure 1.

For $E = 0$ experimental data and computed expectations agree in the whole temperature range for both heating and cooling runs with remarkable accuracy [17]. For $E \neq 0$ and cooling runs data also agree well. It should be pointed out here that it was the applied electric field that was introduced in the algorithm used for computing $\Delta c(T, E)$, i.e. no fit is needed to obtain this computed expectation. Hence, the agreement between expectations and experimental data shows that the paraelectric to ferroelectric phase transition is well described by the Landau theory.

On the contrary, data on heating runs and $E \neq 0$ show deviations in the ferroelectric phase, especially close to the transition temperature where the specific heat sharply increases. Generally, experimental data are found to be less than computed expectations. Taking into account that the experimental values are lower than the predicted curve and that the electric field decreases Δc at each temperature, the effect on the specific heat would be similar to that of an effective field (higher than the applied field) acting on the sample. A similar behaviour was previously found for specific heat in TGSe under electric fields lower than $E < 175$ V cm^{-1}, including the fact that the influence of the electric field becomes more significant on the ferroelectric to paraelectric phase transition [21].

4.3. Latent heat

In a first order phase transition, the temperature at which the transition takes place is not predetermined. When cooling the sample, the high temperature phase could be supercooled below $T_{\rm tr}$. Fluctuations could now trigger the phase transition at any temperature ranging from $T_{\rm tr}$ to $T_{\rm c}$, which is the lower bound of stability for the high temperature phase. Then, the experimental latent heat depends on the temperature at which a transition actually takes place since the discontinuity in P^2 (and in entropy excess) changes with the transition temperature (see figure 4). Similar behaviour is found for heating experiments where the low temperature phase could be superheated above $T_{\rm tr}$ and the transition is triggered anywhere from $T_{\rm tr}$ to T_2, also giving a range of latent heat values.

The theoretical dependence of the latent heat as a function of the temperature at which the transition actually takes place, ($T_{\rm exp}$), for $E = 400$ and 800 V cm^{-1} was computed. To do this, P^2 was obtained from equation (2) for both phases under the selected applied electric field (see figure 4) and the corresponding discontinuity $P_{\rm exp}^2$ was computed as a function of the transition temperature. Latent heat is then obtained from the entropy discontinuity as follows:

$$L = T_{\rm exp}\Delta S_{\rm exp} + \Delta G = -T_{\rm exp}\tfrac{1}{2}\alpha P_{\rm exp}^2 + \Delta G. \tag{11}$$

In this equation ΔG will be equal to zero at T_{tr} and non-zero elsewhere. Anyway, ΔG is much lower than $T\Delta S$ and can be discarded in computations.

Figure 5 shows the results of this calculation for $E = 400$ and $E = 800$ V cm^{-1}. The latent heat changes smoothly with the transition temperature. Interestingly, there is a wide range of allowed values for L, both from T_{tr} to T_c (cooling) and from T_{tr} to T_2 (heating).

Experimental latent heat data shown in table 1 are also plotted in figure 5 for the sake of comparison. L_c data are in agreement with the range of allowed values for the latent heat under an electric field. It should again be pointed out that no fitting was made on figure 5, so that it clearly shows an agreement between experimental data and theoretical expectations when coming from the paraelectric phase.

In contrast, experimental latent heats on heating runs L_h are lower than the lowest theoretical value (corresponding to $L_h(T_2)$), showing that the 2-4-6 Landau potential under an electric field does not describe the experimental value for the discontinuity on the ferroelectric–paraelectric phase transition. However, taking into account that the higher the electric field the less latent heat, the experimental data on L_h (lower than the expected theoretical values) could be compatible with the hypothesis of the existence of an effective electric field higher than the applied one.

4.4. Susceptibility

Finally, experimental data for dielectric susceptibility will be compared to the theoretical prediction given by

$$\chi^{-1} = \varepsilon_0 \left(\frac{\partial^2 \Delta G}{\partial P^2} \right) = \varepsilon_0 \frac{1}{\alpha(T - T_c) + 3\beta P^2 + 5\gamma P^4}. \quad (12)$$

The theoretical χ as a function of electric field is deduced in a similar way to that previously used for specific heat excess. The theoretical behaviour is also included in figure 3. It is remarkable that the predictions for stable regions and experimental data are in full agreement. For $E = 400$ V cm^{-1} there are deviations for ferroelectric to paraelectric phase transition data near the maximum of the anomaly in the metastable region. For $E = 800$ V cm^{-1} there are deviations for both cooling and heating data, also in the metastable region. It should be taken into account that it was the adiabatic susceptibility that was measured, while the theoretical prediction is only valid for the isothermal susceptibility. Some differences are then expected near the transition temperature. Drawing additional conclusions for the dielectric susceptibility is not straightforward because it is very sensitive to phase front propagation, domain growth and destruction processes [23–26].

5. Discussion

Specific heat, latent heat and dielectric susceptibility have been measured under an electric field of $E = 400$ and 800 V cm^{-1} in 90% deuterated TGSe single crystal.

When the sample undergoes the transition from the paraelectric to the ferroelectric phase, the 2-4-6 Landau potential for $E = 0$ plus the classical term $-EP$ successfully describe the temperature dependence of those quantities. Furthermore, the experimental transition temperature and the theoretical phase diagram agree. It is remarkable that no data were fitted or adjusted in the computation, so that the predictions of the Landau theory and experiments are in full agreement.

The Landau theory and experiments were also previously found to agree well for the specific heat anomaly of the second order phase transition in TGS [2], for $E > 300$ V cm^{-1}, and for the first order phase transition in KDP [5], for $E > 360$ V cm^{-1}, above the critical field (no latent heat being developed). In the same way this work puts forward an excellent correlation between theory and experiments for the first order phase transition in 90% deuterated TGSe, showing that the phenomenological theory is valid when the transition goes from the paraelectric phase to the ferroelectric one. No

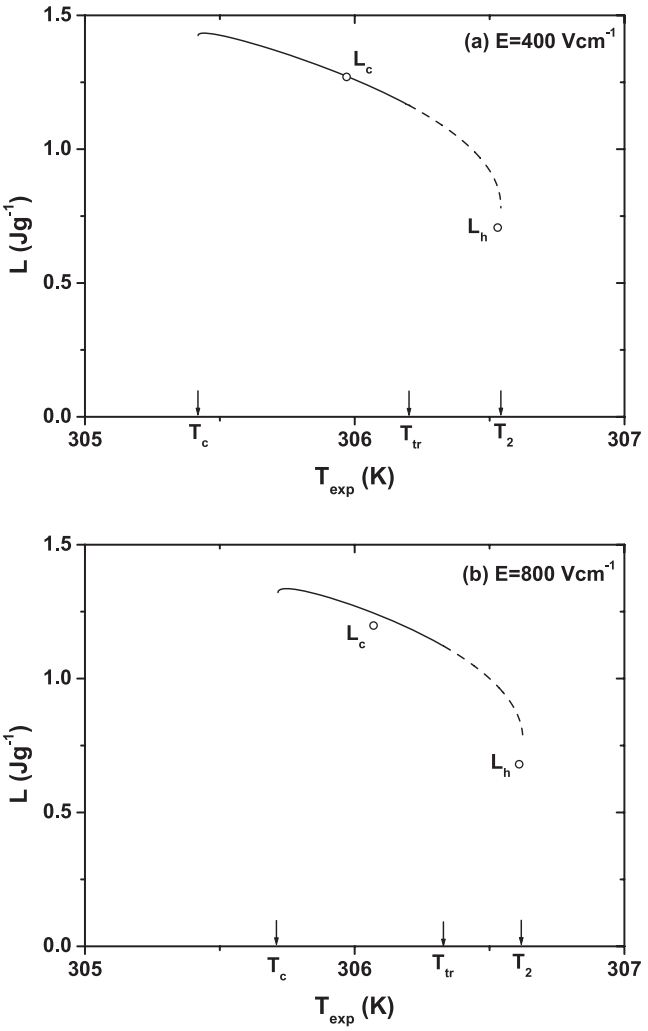

Figure 5. Calculated latent heat (see equation (11)) as a function of the temperature at which the transition takes place (T_{exp}) for (a) $E = 400$ V cm^{-1} and (b) $E = 800$ V cm^{-1}. Allowed values are shown as a solid line (paraelectric to ferroelectric phase transition) and dashed line (ferroelectric to paraelectric). Experimental latent heat values on cooling runs (L_c) and on heating runs (L_h) (open circles in both cases) are also shown.

similar study for thermal and dielectric properties for any other material with a first order phase transition, under electric fields lower than the critical one, can be found in the literature to the best of our knowledge.

If scanning goes from the ferroelectric to the paraelectric phase, specific heat and latent heat data are lower than the predictions of Landau theory. The electric field moves the transition temperature to the upper limit of stability, although the experimental values lie within the theoretical expectations (see figure 2). It cannot be straightforwardly explained why the ferroelectric phase is superheated up to T_2 while the paraelectric phase is not supercooled down to T_c, despite both heating and cooling runs being carried out at the same rate of temperature change.

In summary, although a 2-4-6 Landau theory under an electric field provides an accurate description of several kinds of data for the paraelectric to ferroelectric phase transition, significant deviations are found in the ferroelectric to paraelectric phase transition in almost fully deuterated TGSe. In this case (ferroelectric to paraelectric phase transition), the full set of data shows that a closer agreement would be found assuming an acting field higher than the applied one.

A similar behaviour was recently reported [4, 21] for tricritical phase transition in TGSe after studying the influence of the electric field on the specific heat. Ferroelectric phase data for $E \neq 0$ were also explained by considering an effective field higher than the applied field. Interestingly, this effective field was remarkably significant for the heating experiments, because the specific heat on this type of run was observed to smear largely, even when applying very low electric fields. In contrast, the specific heat anomaly for the corresponding cooling run did not show that smearing. Hence, on heating runs, even very low applied fields seemed to trigger large effective fields on this sample.

A similar behaviour was also found recently for ferroelectric MAPCB and MAPBB [27] where scaling laws for dielectric susceptibility describe experimental data if an effective field different from the applied field is considered.

This behaviour could be related to non-equilibrium processes not described by the phenomenological theory. As an example it should be considered that, in the ferroelectric phase, the total energy of the crystal is minimized by setting the appropriate domain configuration. Morphology and reorientation dynamics of domains also change the electric, mechanic and optical properties of ferroelectric materials. The resulting domain dynamics depends on the temperature, the applied field and the presence of point defects, which could help to create local electric fields [28].

For paraelectric to ferroelectric phase transitions, the phenomenological theory gives an excellent description of experimental data showing that the above mentioned effects are not significant during domain growth in the ferroelectric phase. When the transition is approached from the ferroelectric phase those effects become significant. This work shows that this influence can also be observed in thermal properties when measuring with high-resolution calorimetry. These results may be influenced by the different dynamic processes of growth and destruction of domains.

Acknowledgments

This work has been supported by project FIS2006-04045 of the Spanish DGICYT. The authors wish to thank Professor José María Martín Olalla for his contribution to the preparation of this manuscript and for fruitful conversations about the content of the paper.

References

[1] Strukov B A, Taraskin S A and Meleshina V A 1970 *Sov. Phys.—Solid State* **12** 1089
[2] Ramos S, del Cerro J and Zamora M 1980 *Phys. Status Solidi* a **61** 307
[3] Strukov B A, Taraskin S A and Varikash V M 1968 *Sov. Phys.—Solid State* **10** 1445
[4] Romero F J, Gallardo M C, Jiménez J and del Cerro J 2005 *J. Phys.: Condens. Matter* **17** 5001
[5] Sandvold E and Fossheim K 1986 *J. Phys. C: Solid State Phys.* **19** 1481
[6] Delgado-Sánchez J M, Martín-Olalla J M, Gallardo M C, Ramos S, Koralewski M and del Cerro J 2005 *J. Phys.: Condens. Matter* **17** 2645
[7] Shnaidshtein I V and Strukov B A 2006 *Phys. Solid State* **48** 2142
[8] Western A B, Baker A G, Bacon C R and Schmidt V H 1978 *Phys. Rev.* B **17** 4461
[9] Courtens E and Gammon R W 1981 *Phys. Rev.* B **24** 3890
[10] Dukek G and Falk G 1970 *Z. Phys.* **240** 93
[11] del Cerro J, Martín-Olalla J M and Romero F J 2003 *Thermochim. Acta* **401** 149
[12] Romero F J, Gallardo M C, Jiménez J, del Cerro J and Salje E K H 2000 *J. Phys.: Condens. Matter* **12** 4567
[13] Romero F J, Gallardo M C, Jiménez J, Koralewski M, Czarnecka A and del Cerro J 2004 *J. Phys.: Condens. Matter* **16** 7637
[14] Gesi K 1976 *J. Phys. Soc. Japan* **41** 565
[15] Aragó C and Gonzalo J A 2000 *J. Phys.: Condens. Matter* **12** 3737
[16] Aragó C and Gonzalo J A 2000 *Ferroelectr. Lett.* **27** 83
[17] Romero F J, Gallardo M C and del Cerro J 2006 *Europhys. Lett.* **76** 863
[18] Gallardo M C, Jiménez J and del Cerro J 1995 *Rev. Sci. Instrum.* **66** 5288
[19] del Cerro J 1988 *J. Therm. Anal.* **34** 335
[20] del Cerro J, Romero F J, Gallardo M C, Hayward S A and Jiménez J 2000 *Thermochim. Acta* **343** 89
[21] Romero F J, Gallardo M C, Jiménez J and del Cerro J 2006 *J. Phys.: Condens. Matter* **18** 10075
[22] Romero F J, Gallardo M C, Czarnecka A, Koralewski M and del Cerro J 2007 *J. Therm. Anal. Calorim.* **87** 355
[23] Bornarel J and Cach R 1991 *Ferroelectrics* **124** 345
[24] Bornarel J and Cach R 1999 *Phys. Rev.* B **60** 3806
[25] Kvitek Z and Bornarel J 2000 *J. Phys.: Condens. Matter* **12** 7819
[26] Bornarel J and Cach R 1999 *J. Phys.: Condens. Matter* **15** 4371
[27] Gaiazka M, Szklarz P, Bator G and Zielinski P 2006 *Phase Transit.* **79** 545
[28] Viehland D and Chen Y H 2000 *J. Appl. Phys.* **88** 6696